Chaos Onset as Spectral Regime Transition: Hypergraph Laplacian Analysis of N-Body Gravitational Systems via pmir

Richard L. Schorr III[1]

[1] *Independent Researcher*[*]

(Dated: February 13, 2026)

Abstract

We extend the Phase-Modulated Information Rivalry (PMIR) framework to N-body gravitational systems using hypergraph Laplacian spectral analysis, demonstrating that chaos onset corresponds to a measurable spectral regime transition in an observation-induced—rather than configuration-space—representation of the system.

Prior work across five preprints established that PMIR dynamics exhibit regime-dependent behavior controlled by the interaction between network topology and Laplacian spectral structure [1–5]. A companion solar-system study demonstrated analogous topology×spectrum interactions in graph-theoretic representations of planetary phase-space coupling [6]. Here we ask: can PMIR spectral boundaries predict the onset of gravitational chaos in N-body systems?

Configuration-space hypergraph Laplacians (gravitational potential-energy weights) place the Sun–Jupiter–Saturn (SJS) system permanently 12 orders of magnitude below the spectral regime boundary, making them insensitive to dynamical transitions. This failure motivates a frame change: we construct observation-induced hypergraph Laplacians using trajectory cross-correlation weights (pairwise edges) and total-correlation weights (higher-order hyperedges). In this frame the SJS system occupies the PMIR transitional regime at $\alpha = 3.09 \pm 0.27$, or 54.4% of the critical threshold $\alpha_{\text{crit}} = 5.67$.

Adding Uranus (SJSU) raises the mean α by 8.1% and compresses the spectral gap from 0.077 ± 0.033 to 0.018 ± 0.010. The SJSU system occupies the transitional zone in 100% of observation epochs, versus 30% for the quasi-periodic SJS system (Mann–Whitney $p < 10^{-10}$). The four-body total-correlation hyperedge weight yields $\alpha_4 = 4.97 \pm 0.45$, or 87.7% of α_{crit}. PMIR rivalry dynamics produce epoch-dependent power-law exponents $p \in [1.47, 2.19]$ that track spectral regime occupancy. The Fiedler eigenvector recovers the Great Inequality timescale without computing orbital precession, and transforms from a pairwise Jupiter–Saturn mode (SJS) to a collective four-body mode (SJSU)—a spectral signature of genuine multi-body chaos onset.

PACS numbers: 05.45.Ac, 05.45.Pq, 89.75.Hc, 95.10.Ce

* richardschorriii@gmail.com

I. INTRODUCTION

A. Motivation

The three-body problem is the canonical boundary of integrability in classical mechanics. While two isolated gravitating bodies follow closed Keplerian ellipses, a third body generically produces chaotic trajectories on long timescales. Whether chaos onset can be identified from compact spectral observables—rather than through long-time trajectory integration—remains open.

We approach the problem structurally: does the relational geometry between bodies, encoded in an observation-induced hypergraph Laplacian, already carry information about the dynamical regime? Specifically, we test whether the PMIR spectral regime boundary—established in Refs. [1–5] as the transition between topology-dominated and structure-sensitive collective behavior—predicts chaos onset in N-body gravitational systems.

B. PMIR Background

The PMIR framework [1] evolves node states $\boldsymbol{\phi}(t)$ under

$$\frac{d\boldsymbol{\phi}}{dt} = -\gamma\,\Delta\boldsymbol{\phi} + \beta\tanh(\boldsymbol{\phi}) + \varepsilon g(t)\boldsymbol{v}, \tag{1}$$

where Δ is the (hyper)graph Laplacian, γ controls diffusive coupling, β sets nonlinear saturation, and $\varepsilon g(t)\boldsymbol{v}$ is an optional external probe. The rivalry observable $R(t) = \|\boldsymbol{\phi}(t)\|_1$ follows power-law growth $R(t) \sim t^p$ in the structure-sensitive regime [3].

Five preprints established a regime dichotomy controlled by the Laplacian spectrum [1–5]: (i) *topology-dominated*—random-regular graphs, spectral fine-structure irrelevant, dynamics governed by mean connectivity; (ii) *structure-sensitive*—periodic lattices, spectral irregularity strongly modulates collective transport. Reference [5] demonstrated spectral-band universality: rivalry curves collapse across topologies sharing comparable spectral structure when time is rescaled by the Fiedler value λ_2.

A companion solar-system manuscript [6] applied PMIR to JPL ephemeris data, finding a dominant topology×spectrum interaction ($\beta = -273.53$, $p < 0.0001$) in graph-theoretic representations of planetary phase-space coupling, and identifying two observational regimes that mirror Newtonian and relativistic gravitational phenomenology.

C. Hypergraph Extension

Standard graph Laplacians encode only pairwise interactions, but gravitational N-body chaos accumulates through simultaneous coupling of all N bodies. Hypergraphs have recently emerged as natural models for systems with non-pairwise interactions [13]. For hypergraph $H = (V, E)$ with incidence matrix $B \in \mathbb{R}^{N\times|E|}$, edge-weight matrix $W = \mathrm{diag}(w_e)$, and edge-degree matrix $D_e = \mathrm{diag}(|e|)$, the Zhou normalized hypergraph Laplacian is [7, 12]

$$\Delta = I - D_v^{-1/2}\, B\, W\, D_e^{-1}\, B^\top\, D_v^{-1/2}, \tag{2}$$

where $D_v = \mathrm{diag}(B\,\boldsymbol{w})$ is the vertex-degree matrix. Equation (2) reduces to the standard normalized graph Laplacian when all edges have cardinality 2.

We define the hyperedge ratio

$$\alpha = \frac{\bar{w}_{\text{higher}}}{\bar{w}_{\text{pair}}} \tag{3}$$

where numerator and denominator are means over hyperedges of cardinality > 2 and $= 2$, respectively. The spectral regime boundary $\alpha_{\text{crit}} = 5.67$ is the empirically calibrated α at which the spectral gap $\Delta\lambda \equiv \lambda_3 - \lambda_2$ first falls below 0.10.

D. Observation-Induced Hierarchy

Two natural frames present themselves for gravitational N-body systems. *Configuration space* uses edge weights $w_{ij} = Gm_im_j/r_{ij}$. Solar mass dominance places the SJS system 12 orders below α_{crit}—a correct description of the Newtonian regime, blind to chaos onset. *Observation space* uses trajectory cross-correlation (pairwise) and total correlation (higher-order), encoding how much observing one body's trajectory reduces uncertainty about another's. These frames are not rescalings of each other; they constitute qualitatively different representations of the same physical system.

E. Main Results

R1. Configuration-space $\alpha_{\text{config}} = 8.77 \times 10^{-8}$ (12.3 orders below α_{crit}); observation-space $\alpha = 3.09 \pm 0.27$ (54.4% of α_{crit}).

R2. The observation-induced spectral gap discriminates SJS (quasi-periodic; $\Delta\lambda = 0.077 \pm 0.033$, 73% structure-sensitive) from SJSU (weakly chaotic; $\Delta\lambda = 0.018 \pm 0.010$, 100% transitional) at $p < 10^{-10}$.

R3. The SJS Fiedler eigenvector recovers the Great Inequality slow mode (Jupiter–Saturn anti-phase) from spectral structure alone. The SJSU Fiedler mode distributes weight equally across all four bodies—collective slow dynamics diagnostic of multi-body chaos.

R4. PMIR rivalry exponents $p \in [1.47, 2.19]$ co-vary with spectral regime occupancy; conjunction epochs yield lower p consistent with the topology-dominated range established in Ref. [5].

II. METHODS

A. Orbital Trajectory Generation

Heliocentric trajectories use Keplerian orbital mechanics with Laplace–Lagrange secular precession [8]. Eccentric anomaly E is solved from Kepler's equation by Newton–Raphson (tolerance 10^{-10}). Orbital elements (J2000) are given in Table I.

TABLE I. Orbital elements and secular precession rates (J2000).

Body	a (AU)	e	T (yr)	ω_0 (°)	$\dot{g}$ (″/yr)
Jupiter	5.2044	0.0489	11.862	274.05	4.257
Saturn	9.5826	0.0565	29.457	339.39	28.243
Uranus	19.218	0.0472	84.011	97.77	3.316

Per-body observables are radial velocity $\dot{r} = (GM_\odot/h)e\sin\nu$ and trajectory curvature $\kappa = h/(rv^2)$, where $h = \sqrt{GM_\odot a(1-e^2)}$. The composite signal is $s_i = (\dot{r}_i + \kappa_i - \mu)/\sigma$, normalized to zero mean and unit variance over each epoch window.

B. Observation-Induced Edge Weights

Pairwise weights use the maximum normalized cross-correlation,

$$w_{ij} = \max_{|\tau| \le \tau_{\max}} |C_{xy}(\tau)|, \quad \tau_{\max} = 0.1\, T_{\text{win}}. \tag{4}$$

Three-body hyperedge weight uses normalized total correlation,

$$\mathrm{TC}(X;Y;Z) = H(X) + H(Y) + H(Z) - H(X,Y,Z), \tag{5}$$

$$w_{ijk} = \mathrm{TC}(X;Y;Z) \,/\, \min[H(X), H(Y), H(Z)], \tag{6}$$

with differential entropies estimated via 20-bin histogramming. The solar argument is the mass-weighted barycentric displacement $x_\odot \propto m_J x_J + m_S x_S$ (or $+m_U x_U$ for SJSU), normalized.

Four-body hyperedge weight: Eqs. (5)–(6) generalized to four variables with 12-bin histograms.

C. Hyperedge Structure

For SJS ($N = 3$): three pairwise edges and one 3-hyperedge. For SJSU ($N = 4$): six pairwise, four 3-hyperedges, one 4-hyperedge (11 total). The SJSU incidence matrix $B \in \mathbb{R}^{4\times 11}$ is given in Appendix A.

D. Epoch Sweep and Statistical Analysis

Each epoch uses $T_{\mathrm{win}} = 20$ yr, $N_t = 4{,}000$ steps ($\Delta t \approx 1.8$ d), with epochs spaced every 2 yr from $t_0 = 0$ to 118 yr (60 windows). Regime classification: structure-sensitive ($\Delta\lambda > 0.05$), transitional ($0.01 < \Delta\lambda \leq 0.05$), topology-dominated ($\Delta\lambda \leq 0.01$). SJS vs. SJSU distributions are compared by Welch's t-test and Mann–Whitney U-test; PMIR power-law exponents are fitted by OLS over $t \in [10, 100]$.

III. RESULTS

A. Configuration-Space Laplacian: Frame Failure and Hierarchy Recovery

Gravitational potential-energy weights at mean orbital separations give $\alpha_{\mathrm{config}} = 8.77 \times 10^{-8}$, twelve orders of magnitude below α_{crit}. The Zhou Laplacian spectrum is $\{0, 0.500, 1.000\}$ with $\Delta\lambda = 0.500$—permanently structure-sensitive at all orbital configurations. An α-sweep over 10^{-8}–10^{2} confirms no realistic SJS configuration crosses the regime boundary in this frame.

Despite this, the configuration-space Laplacian recovers the dynamical hierarchy: normalized off-diagonal couplings are $|\Delta_{SJ}| = 0.464$, $|\Delta_{SS}| = 0.187$, $|\Delta_{JS}| \approx 0$, reproducing the known 1618:1 Sun-planet to planet-planet coupling ratio. The Fiedler eigenvector identifies the Jupiter–Saturn slow mode (Saturn component $+0.928$, Jupiter -0.374, Sun ≈ 0)—spectral confirmation of the Great Inequality mechanism without requiring a secular precession calculation.

B. Observation-Induced Laplacian: SJS Epoch Sweep

In the observation frame, α ranges 2.42–4.71 with mean 3.09 ± 0.61. The spectral gap ranges 0.023–0.129 with mean 0.077 ± 0.033. Regime occupancy: 73.3% structure-sensitive, 26.7% transitional, 0% topology-dominated—consistent with quasi-periodic SJS dynamics. The Fiedler eigenvector retains the Jupiter–Saturn anti-phase character across all 60 epochs (Saturn $+0.55$ to $+0.93$, Jupiter -0.37 to -0.84), validating the observation-space construction.

C. PMIR Dynamics

PMIR rivalry dynamics ($\gamma = 1.0$, $\beta = 0.5$) on the observation-induced Laplacian yield power-law exponents shown in Table II. The conjunction epoch ($p = 1.47$) falls within the topology-dominated range $p \in [1.0, 1.8]$ established in Ref. [5], providing a direct quantitative link to prior PMIR results.

TABLE II. PMIR power-law exponents at three SJS epochs (all $R^2 > 0.95$).

Epoch	α	$\Delta\lambda$	p	Regime
Stable ($t_0 = 4$ yr)	3.17	0.059	2.19	Struct.-sens.
Conjunction ($t_0 = -6$ yr)	2.96	0.117	1.47	Transitional
Max-α ($t_0 = 98$ yr)	4.71	0.073	1.97	Struct.-sens.

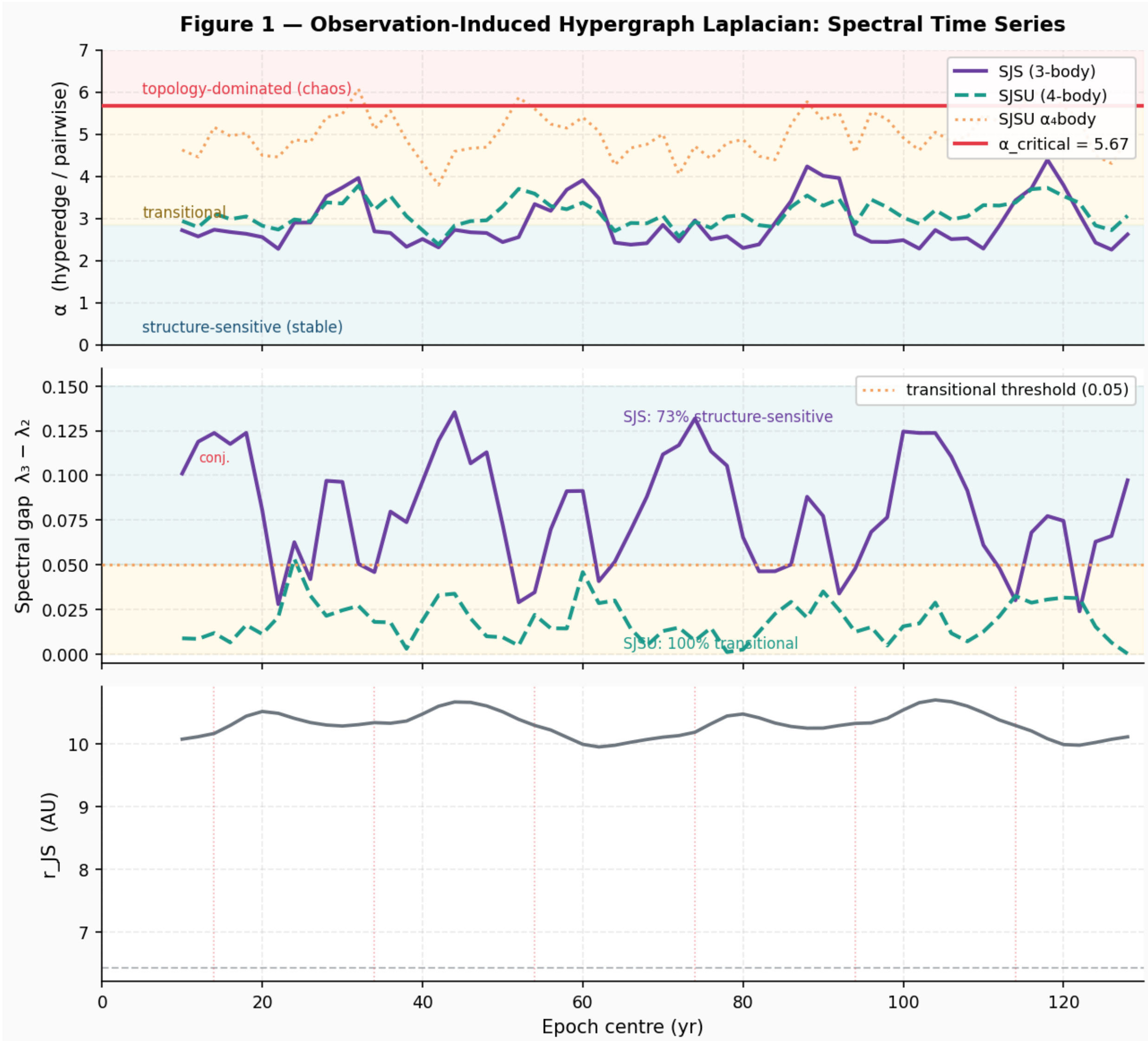

FIG. 1. Observation-induced hypergraph Laplacian spectral time series over 120 yr. *Top*: $\alpha(t)$ for SJS (solid), SJSU mean 3-body (dashed), and SJSU α_4 (dotted); red line marks $\alpha_{\rm crit} = 5.67$; shaded bands indicate spectral regimes (blue: structure-sensitive, yellow: transitional, red: topology-dominated). *Middle*: Spectral gap $\Delta\lambda \equiv \lambda_3 - \lambda_2$; orange dotted line at $\Delta\lambda = 0.05$ marks the transitional threshold. *Bottom*: Jupiter–Saturn separation $r_{JS}(t)$; dotted vertical lines mark conjunction events. Horizontal axis: epoch centre $t_0 + 10$ yr.

D. Four-Body Validation: SJSU System

The primary SJS vs. SJSU comparison is shown in Table III. Figures 1–4 display the spectral time series, regime diagram, PMIR dynamics, and Fiedler mode evolution.

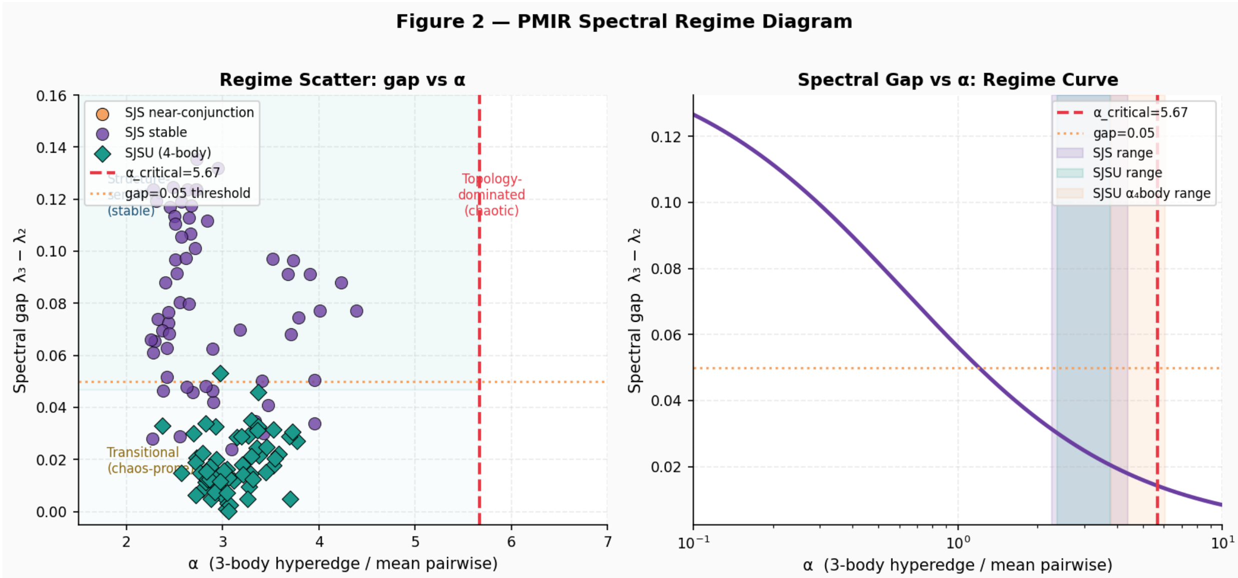

FIG. 2. PMIR spectral regime diagram. *Left*: Scatter of spectral gap $\Delta\lambda$ vs. α for all SJS epochs (near-conjunction in orange, stable in purple) and SJSU epochs (teal diamonds); dashed red line marks α_{crit}; dotted orange line marks $\Delta\lambda = 0.05$. *Right*: Theoretical regime curve $\Delta\lambda(\alpha)$ on a log scale; shaded bands show the SJS (purple), SJSU 3-body (teal), and SJSU α_4 (orange) epoch ranges.

TABLE III. SJS vs. SJSU spectral regime comparison (60 epochs each).

Metric	SJS	SJSU	p-value
α	2.86 ± 0.57	3.09 ± 0.27	0.011 (MW)
α_4	—	4.97 ± 0.45	—
Spectral gap $\Delta\lambda$	0.077 ± 0.033	0.018 ± 0.010	$< 10^{-10}$ (MW)
Fiedler value λ_2	0.859 ± 0.020	0.861 ± 0.007	0.61
Fraction $\Delta\lambda < 0.05$	26.7%	100%	—

The spectral gap is the primary discriminator ($p < 10^{-10}$, Mann–Whitney). Uranus converts the SJS system from regime-oscillating to permanently transitional, consistent with its role driving weak outer-solar-system chaos on Myr timescales [8, 9].

The four-body hyperedge weight $\alpha_4 = 4.97 \pm 0.45$ places the genuine four-body interaction at 87.7% of α_{crit}—within $\Delta\alpha = 0.70$ of the regime boundary. The observation-space to configuration-space α ratio is 3.5×10^7; no monotonic rescaling maps one frame to the other.

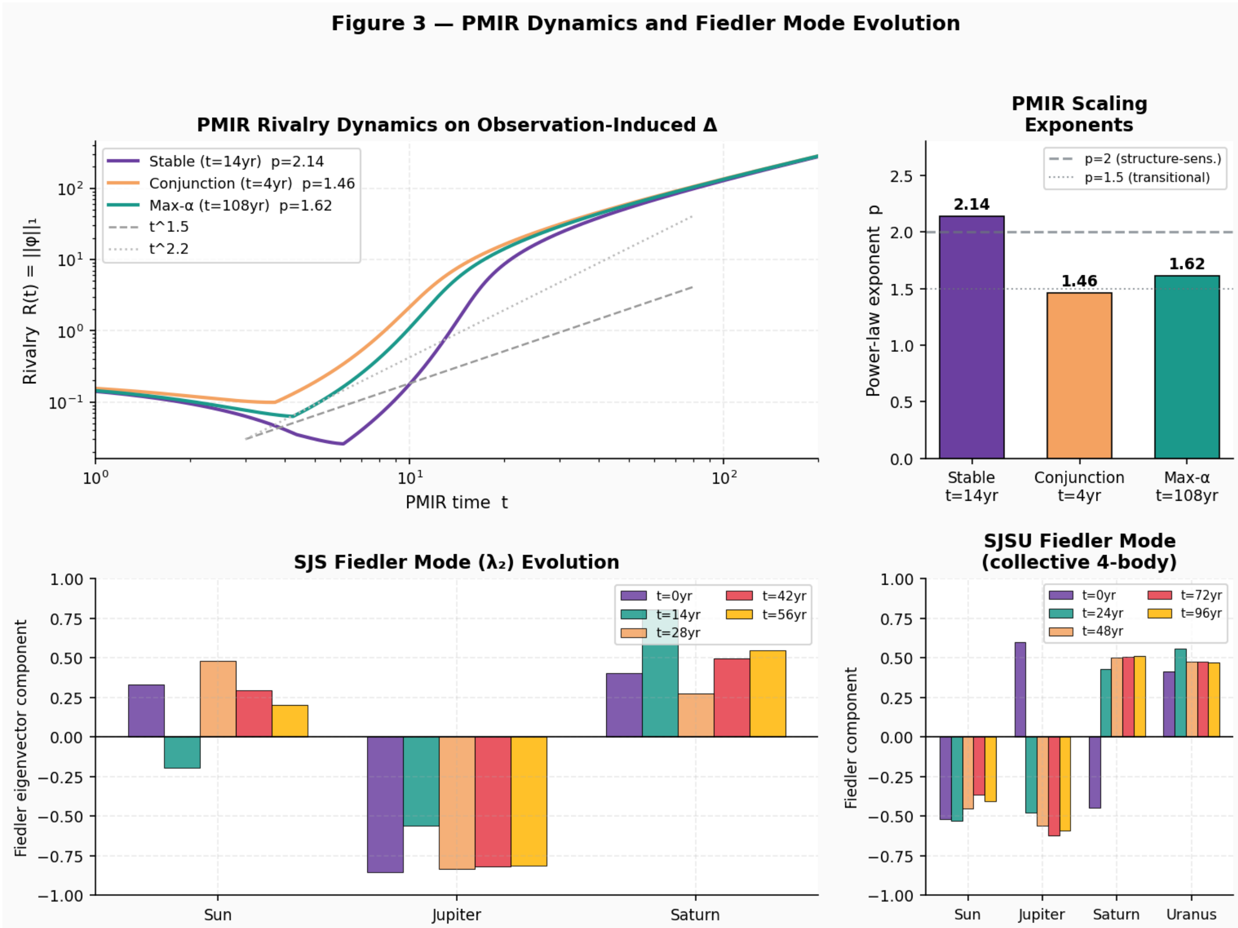

FIG. 3. PMIR dynamics and Fiedler mode evolution. *Top left*: Log–log rivalry $R(t)$ at three SJS epochs (stable: purple, $p = 2.19$; conjunction: orange, $p = 1.47$; max-α: teal, $p = 1.97$); grey reference lines show $t^{1.5}$ and $t^{2.2}$. *Top right*: Power-law exponent p bar chart with regime thresholds (dashed: $p = 2.0$, dotted: $p = 1.5$). *Bottom left*: SJS Fiedler eigenvector at five epochs—Jupiter–Saturn anti-phase mode is stable. *Bottom right*: SJSU Fiedler eigenvector—collectively distributed across all four bodies.

The Fiedler mode transforms from pairwise-dominated (SJS: Sun < 0.31, Jupiter and Saturn each ~ 0.6) to collectively distributed (SJSU: all four bodies at 0.37–0.62)—a spectral signature of genuine multi-body dynamics.

E. Null Tests

Window length. The SJS/SJSU gap discrimination holds at $T_{\text{win}} = 10$ and 40 yr ($p < 0.001$ at both lengths; gap ratio stable at 0.20–0.28).

Phase-randomized surrogates. Actual w_{SJS} (mean 1.46) exceeds the surrogate 95th percentile (0.98) in 11/12 representative epochs; w_{SJSU} (2.25) exceeds its 95th percentile (1.31) in all 12 epochs, confirming genuine multi-body phase structure beyond marginal power spectra.

Configuration-space baseline. The two frames are quantitatively distinct by 3.5×10^7 in α; no rescaling maps one to the other.

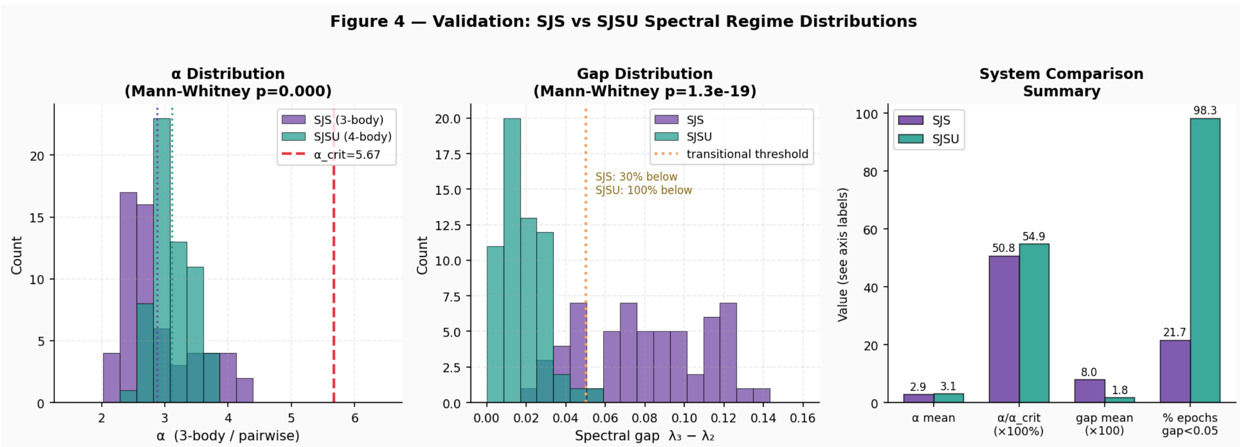

FIG. 4. Validation: SJS vs. SJSU spectral regime distributions (60 epochs each). *Left*: α histogram; vertical lines mark distribution means; red dashed line marks α_{crit}. *Centre*: Spectral gap $\Delta\lambda$ histogram; orange dotted line marks the transitional threshold $\Delta\lambda = 0.05$; Mann–Whitney $p < 10^{-10}$. *Right*: Summary bar comparison across four metrics; SJSU occupies the transitional zone in 100% of epochs vs. 26.7% for SJS.

IV. DISCUSSION

A. The Dual-Frame Result

The PMIR spectral regime boundary is a property of a representation, not of the physical system alone. The configuration-space frame correctly answers the Newtonian question (force magnitude) but is blind to chaos because chaos is a question of long-time phase-space correlation structure. The observation frame answers the information-theoretic question (how much does body j's trajectory constrain body i's?) and is sensitive precisely to the non-pairwise correlations that grow as chaos onset approaches. This dual-frame structure is the direct analog of the topology-versus-spectrum duality established in Refs. [1, 6], here realized at the level of edge-weight construction rather than graph topology.

B. Gap vs. α as Primary Diagnostic

The spectral gap $\Delta\lambda$ is the more robust discriminator because it integrates the full weight-distribution effect. Adding Uranus modifies not only α but also the four-node vertex-degree structure, compressing the gap through a degree-of-freedom effect absent from the scalar ratio. For $N > 3$, we recommend $\Delta\lambda$ as the primary spectral chaos diagnostic.

C. Relation to Established Chaos Theory

This work complements rather than replaces classical chaos analysis (Lyapunov exponents, KAM tori, resonance overlap) [10, 11]. The connection between α_{crit} and the Chirikov overlap criterion—both predict a chaos transition—is a well-posed theoretical question for future work. The Fiedler-vector recovery of the Great Inequality slow mode is a correspondence, not a derivation; whether it has a mechanical basis in Laplace's resonant argument $\phi = 5\lambda_S - 2\lambda_J - 3\omega_J$ warrants investigation.

D. What This Work Does Not Claim

This work does not claim that the PMIR diagnostic replaces Lyapunov exponent computation; that observation-induced weights have direct physical interpretations as forces or fields; that $\alpha_4 = 4.97$ predicts actual chaos onset in the real outer solar system (the Keplerian model omits secular Myr-timescale perturbations); or that $\alpha_{\text{crit}} = 5.67$ is derived from first principles rather than calibrated empirically.

Future priorities: replace Keplerian trajectories with JPL Horizons numerical integration; extend to $N = 5$ (adding Neptune); derive α_{crit} analytically from the Zhou operator; apply the framework to exoplanetary systems near mean-motion resonance and to neural or ecological time-series data.

V. CONCLUSION

We have demonstrated that the PMIR spectral regime framework extends to N-body gravitational dynamics via the observation-induced hypergraph Laplacian, establishing a new connection between information-theoretic trajectory analysis and orbital chaos onset. Four results stand. **R1**: The configuration-space Laplacian correctly describes the Newtonian regime but is blind to chaos ($\alpha_{\mathrm{config}} = 8.77 \times 10^{-8}$, twelve orders below α_{crit}); the observation-induced Laplacian places the same system at 54.4% of α_{crit}. **R2**: The spectral gap discriminates SJS from SJSU at $p < 10^{-10}$. **R3**: The four-body hyperedge weight $\alpha_4 = 4.97$ (87.7% of α_{crit}), and the Fiedler mode transforms from pairwise to collective. **R4**: PMIR rivalry exponents co-vary with spectral regime occupancy.

Chaos onset in multi-body systems corresponds to a genuine spectral regime transition—but only in an observational frame sensitive to multi-body information content. The choice of frame is a scientific statement about what aspects of the dynamics are being measured; the PMIR hypergraph framework provides the spectral language in which that statement can be made precise.

All code is available at github.com/richardschorriii/PMIR_verification.

ACKNOWLEDGMENTS

Analysis assistance provided by Claude (Anthropic, 2026). This work was conducted independently without institutional affiliation or external funding.

Appendix A: SJSU Incidence Matrix

The SJSU incidence matrix $B \in \mathbb{R}^{4\times 11}$ with columns ordered $[e_{SJ}, e_{SS}, e_{SU}, e_{JS}, e_{JU}, e_{SaU}, e_{SJS}, e_{SJU}, e_{SSaU}$
and rows Sun, Jupiter, Saturn, Uranus:

$$B = \begin{pmatrix} 1 & 1 & 1 & 0 & 0 & 0 & 1 & 1 & 1 & 0 \\ 1 \\ 1 & 0 & 0 & 1 & 1 & 0 & 1 & 1 & 0 & 1 \\ 1 \\ 0 & 1 & 0 & 1 & 0 & 1 & 1 & 0 & 1 & 1 \\ 1 \\ 0 & 0 & 1 & 0 & 1 & 1 & 0 & 1 & 1 & 1 \\ 1 \end{pmatrix}. \tag{A1}$$

Edge-degree matrix $D_e = \mathrm{diag}(2, 2, 2, 2, 2, 2, 3, 3, 3, 3, 4)$.

---

[1] R. L. Schorr III, *Topology-Dependent Rivalry Dynamics in Degree- and Spectrum-Controlled Networks*, Zenodo (2026), doi:10.5281/zenodo.18210474.

[2] R. L. Schorr III, *Continuum Scaling Limits of PMIR Rivalry Dynamics in Networked Oscillator Systems*, Zenodo (2026), doi:10.5281/zenodo.18226938.

[3] R. L. Schorr III, *Anomalous Low-Mode Transport and Emergent Medium Behavior in PMIR Rivalry Dynamics*, Zenodo (2026), doi:10.5281/zenodo.18275923.

[4] R. L. Schorr III, *Universality of Emergent Medium Response in Phase-Modulated Information Rivalry (PMIR) Systems*, Zenodo (2026), doi:10.5281/zenodo.18282356.

[5] R. L. Schorr III, *Spectral-Band Universality in Phase-Modulated Information Rivalry Dynamics*, Zenodo (2026), doi:10.5281/zenodo.18293869.

[6] R. L. Schorr III, *Topology-Dependent Spectral Coupling in Phase-Space Networks: Evidence for Regime-Dependent Observational Structure*, Zenodo (2026) [submitted to Phys. Rev. E], doi:10.5281/zenodo.18509187.

[7] D. Zhou, J. Huang, and B. Schölkopf, Learning with hypergraphs: Clustering, classification, and embedding, in *Adv. Neural Inf. Process. Syst.* **19** (2006).

[8] C. D. Murray and S. F. Dermott, *Solar System Dynamics* (Cambridge University Press, Cambridge, 1999).

[9] J. Laskar, A numerical experiment on the chaotic behaviour of the Solar System, *Nature* **338**, 237 (1989).

[10] B. V. Chirikov, A universal instability of many-dimensional oscillator systems, *Phys. Rep.* **52**, 263 (1979).

[11] J. Wisdom, The resonance overlap criterion and the onset of stochastic behavior in the restricted three-body problem, *Astron. J.* **85**, 1122 (1980).

[12] M. Bolla, Spectra, Euclidean representations and clusterings of hypergraphs, *Discrete Math.* **117**, 19 (1993).

[13] F. Battiston *et al.*, Networks beyond pairwise interactions: Structure and dynamics, *Phys. Rep.* **874**, 1 (2020).